Efavirenz is predicted to accumulate in brain tissue: an *in silico, in vitro and in vivo* investigation

Paul CURLEY[1], Rajith K R RAJOLI[1], Darren M MOSS[1], Neill J LIPTROTT[1+2], Scott LETENDRE[3], Andrew OWEN[1+2 #] and Marco SICCARDI[1]

[1] Molecular and Clinical Pharmacology, Institute of Translational Medicine, University of Liverpool, Liverpool, UK

[2] European Nanomedicine Characterisation Laboratory, Molecular and Clinical Pharmacology, Institute of Translational Medicine, University of Liverpool, Liverpool, UK

[3] Departments of Medicine and Psychiatry, University of California San Diego, 220 Dickinson Street, Suite A, San Diego, CA 92103, USA.

[*] **Author for correspondence and reprints**:Prof A Owen, Molecular and Clinical Pharmacology, Institute of Translational Medicine, University of Liverpool, UK
Tel: +44 (0) 151 794 8211
Fax: + 44 (0) 151 794 5656
E-mail: aowen@liverpool.ac.uk

Word Count: 3439
References: 34
Figures: 3
Tables: 2
Key words: efavirenz, PBPK, CNS and toxicity
Running (short) Title: Efavirenz Accumulation in Brain Tissue

Abbreviations: cisterna magna (CM), extra cellular fluid (ECF), intracellular space (ICS), left ventricle (LV), nevirapine (NVP), permeability surface area product (log PS), physiologically based pharmacokinetic (PBPK), rapid equilibrium dialysis (RED), sub arachnoid space (SAS), third and fourth ventricles (TFV), van der Waals polar surface area (TPSA) and van der Waals surface area of the basic atoms (vas_{base}).

Abstract

Introduction: Adequate concentrations of efavirenz in the central nervous system (CNS) are necessary to supress viral replication but high concentrations may increase the likelihood of CNS adverse drug reactions. The aim of this investigation was to evaluate efavirenz distribution into the cerebrospinal fluid (CSF) and brain using a physiologically based pharmacokinetic (PBPK) simulation for comparison with rodent and human data.

Methods: Efavirenz CNS distribution was calculated using a permeability-limited model in a virtual cohort of 100 patients receiving efavirenz (600 mg once-daily). Simulations were then compared with human data from the literature and rodent data. Wistar rats were administered with efavirenz (10 mg kg^{-1}) once daily over 5 weeks. Plasma and brain tissue was collected for analysis via LC-MS/MS.

Results: Median C_{max} was predicted to be 3184 ng mL^{-1} (IQR 2219-4851), 49.9 ng mL^{-1} (IQR 36.6-69.7) and 50,343 ng mL^{-1} (IQR 38,351-65,799) in plasma, CSF and brain tissue respectively, tissue to plasma ratio 15.8. Following 5 weeks of oral dosing of efavirenz (10 mg kg^{-1}), the median plasma and brain tissue concentration in rats was 69.7 ng mL^{-1} (IQR 44.9 – 130.6) and 702.9 ng mL^{-1} (IQR 475.5 – 1018.0) respectively, median tissue to plasma ratio was 9.5 (IQR 7.0 – 10.9).

Conclusion: Although useful, measurement of CSF concentrations may be an underestimation of the penetration of antiretrovirals into the brain. Limitations associated with obtaining tissue biopsies and paired plasma and CSF samples from patients make PBPK an attractive tool for probing drug distribution.

Introduction

Despite its widespread use, patients receiving efavirenz-containing therapy frequently report central nervous system (CNS) disturbances. Symptoms of efavirenz-associated adverse drug reactions (ADRs) occur with a high frequency and can include depression, anxiety, abnormal dreams and hallucinations (1). The majority of patients report development of CNS disorders shortly after commencing efavirenz therapy with symptoms dissipating during the initial months of therapy. A minority of patients continue to experience symptoms for the duration of efavirenz use (2). More recently, efavirenz CNS ADRs have been shown to have more long-term effects (3).

In addition to the negative impact on the quality of the patient's life, CNS ADRs may also lead to a decrease in patient adherence. Poor patient adherence to antiretroviral medication is a major concern, in particular drugs displaying a low genetic barrier to resistance such as efavirenz (4). The impact of CNS side effects on patient adherence is not clearly defined. Some previous studies indicate that patients demonstrate tolerance to CNS side effects with minimal impact on patient adherence (5, 6). However, a recent study demonstrated 60% of patients reported CNS side effects as the primary reason for discontinuation vs. 3% of patients receiving alternative antiretroviral therapies (3).

There is a paucity of information regarding distribution of efavirenz into brain tissue. Due to impracticalities in obtaining brain tissue from patients, some groups have used concentrations in cerebrospinal fluid (CSF) as a surrogate for brain concentrations. The majority of pharmacokinetic (PK) studies have focused on describing efavirenz plasma concentrations and elucidating genetic factors that contribute to the variability in efavirenz PK or genetic associations to predict patients at risk of developing CNS toxicity (1, 7, 8). However there are a few small studies that investigated efavirenz PK in both plasma and CSF. CSF concentrations have been shown to be much lower (around 0.5%) than plasma. However, even at 0.5% of the plasma concentration efavirenz concentrations in the CSF exceed the IC_{50} of efavirenz for wild type HIV (9).

The appropriateness of CSF concentrations as a surrogate for brain concentrations is currently the subject of debate (10-12). It has been demonstrated in guinea pigs that brain tissue concentrations of nevirapine (NVP) not only differ from those in the CSF but also vary between brain regions (10). NVP uptake was shown to be 0.32 mL g^{-1} in the CSF whereas NVP uptake was lower in the choroid plexus (0.25 mL g^{-1}) and higher in the pituitary (1.61 mL g^{-1}) when compared to the CSF (10). Indeed, concentrations within CSF have been shown to vary depending on where the sample was taken for other antiretroviral drugs. Lamivudine has been shown to be 5-fold higher in CSF sampled from the lumbar region compared to ventricular CSF in rhesus monkeys (11). Although there are no comparable data for efavirenz in the literature, these data exemplify the challenges associated with predicting brain tissue concentrations in CSF.

PBPK modelling is a bottom up approach to simulate drug distribution in virtual patients. The approach mathematically describes physiological and molecular processes defining PK, integrating drug-specific properties (such as logP, Caco-2 apparent permeability and affinity for transporters and metabolic enzymes) and patient-specific factors (such as height, weight, sex, organ volumes and blood flow) (13). The model presented here is based on a full body PBPK model, supplemented with a 6-compartment model of the CNS and CSF as previously described (14).

The aim of this investigation was to evaluate efavirenz distribution into the CSF and brain using PBPK. Simulated efavirenz PK data were then compared to available experimental data from rodents and clinical data from humans.

Materials & Methods

Animals and treatment

Male Wistar rats (Charles River UK) weighing 180 – 220 g on arrival were used for PK analysis of efavirenz. Food and water were provided *ad libitum*. Following completion of the dosing all animals were sacrificed using an appropriate schedule 1 method (via exposure to CO_2 in a rising concentration). All animal work was conducted in accordance with the Animals (Scientific Procedures) Act 1986 (ASPA), implemented by the United Kingdom Home Office.

Drug Treatment

Eight male Wistar rats were dosed with efavirenz (10 mg kg^{-1}, 2 mL kg^{-1} 0.5% methylcellulose in dH_2O) based on individual weight taken prior to dosing. The selected dose was based on scaling down the dose administered to adult humans (600mg once daily given to an adult weighing 60/70kg). The dose was also selected as it has been administered to rats previously in a study examining the anxiogenic effects where it was shown to induce anxiety in Wistar rats (15). Dosing was administered once daily *via* oral gavage over 5 weeks. The animals were terminated (via exposure to CO_2 in a rising concentration) 2 hours after the final dose and blood was collected *via* cardiac puncture. Blood samples were centrifuged at 2000g for 10 minutes at 4°C to separate plasma. Plasma was immediately frozen at -80°C and stored for later analysis. Brain tissue was also collected and following washing in phosphate buffered saline for 30 seconds 3 times, immediately stored at -30°C for analysis.

Rapid Equilibrium Dialysis

The protein binding of efavirenz in brain tissue was performed using rapid equilibrium dialysis (RED) as described by Liu *et al.* (16). Untreated rat brain tissue was homogenised in 2 volumes (W:V) of 1% saline solution. Since efavirenz is highly protein bound, a dilution of brain tissue (10% and 20% brain tissue were prepared with 1% phosphate buffered saline [PBS]) was used. 200 µl of brain homogenate was spiked with 5000 ng mL^{-1} efavirenz and added to the donor chamber. The receiver chamber contained 350 µl of Sorensons buffer. The RED plate (Thermo, UK) was then placed in a shaking incubator for 4 hours at 37°C at 100 rpm. 250 µl were removed from the receiver

chamber and frozen at -80°C for analysis. The fraction of drug unbound (fu) in brain tissue was then calculated from the diluted brain tissue using the following formula (17):

$$Undiluted\ fu = \frac{\left(\frac{1}{D}\right)}{\left[\frac{1}{fu(apparent)} - 1\right] + \left(\frac{1}{D}\right)}$$

Where fu = fraction unbound and D = dilution factor.

Sample preparation for bioanalysis

Efavirenz was extracted by protein precipitation. 20µl of internal standard (lopinavir 1000ng mL^{-1}) was added to 100µl of sample, standard or QC which was then treated with 400µl of ACN. Samples were then centrifuged at 4000g for 10 minutes at 4°C. The supernatant fraction was transferred to a fresh glass vial and evaporated, samples were placed in a rotary vacuum centrifuge at 30°C and then reconstituted in 140 µl of H_2O:ACN (60:40). 100µl of the sample was then transferred into 200µl chromatography vials. 5µl of each sample was injected for analysis by LC-MS/MS.

Rat brain tissue was homogenised in 3 volumes (W:V) of plasma for 1 minute at maximum power using a Minilys® homogeniser (Bertin technologies, FR). Extraction was performed using protein precipitation detailed in the previous section. Recovery was tested at 3 levels (400 ng mL^{-1} 100 ng $mL^{-1}$and 20 ng mL^{-1}). Mean recovery was 95% (standard deviation 8.9) and 91% (standard deviation 7.8) for plasma and brain, respectively. Samples generated from the RED experiment were pretreated with 20% ACN (PBS and Sorensons buffer were spiked with 20% ACN in order to aid efavirenz solubility in these matrices) and mean recovery was 84% (SD% 11.6).

Quantification of Efavirenz

Quantification was achieved via LC-MS/MS (TSQ Endura, Thermo Scientific) operating in negative mode. The following ions were monitored for quantification in selected reaction monitoring scan: efavirenz (m/z 315 > 242.1, 244.0 and 250.0) and internal standard, lopinavir (m/z 627 > 121.2, 178.1 and 198.1). A stock solution of 1 mg mL^{-1} efavirenz was prepared in methanol and stored at 4°C until use. A standard curve was prepared in plasma by serial dilution from 500 ng mL^{-1} to 1.9 ng mL^{-1} and an additional blank solution was also used.

Chromatographic separation was achieved using a multi step gradient with a Hypersil gold C-18 column (Thermo scientific) using mobile phases A (100% H_2O, 5mM NH_4HCO_2) and B (100% ACN, 5mM NH_4HCO_2). Chromatography was conducted over 8.55 minutes at a flow rate of 300 µl min^{-1}. At the start of each run, mobile phase A was 90% until 0.1 minutes when mobile phase B was increased to 86% at 0.5 minutes. Mobile phase B was then gradually increased to 92% over 4.5 minutes. Mobile phase B was then increased to 97% at 5.1 minutes which was held until 6 minutes. Mobile phase A was then increased to 90% and held till the termination of the run at 8 minutes. Inter- and intra- assay variance in accuracy and precision were <15%.

PBPK parameters

The full body PBPK model used here has been previously published using equations from the physB model (Figure 1) (13, 18). The model generates virtual patients based on a statistical description of human anatomy. The model simulates flow rates, organ volumes and other tissue volumes based on anthropometric measures and allometric scaling.

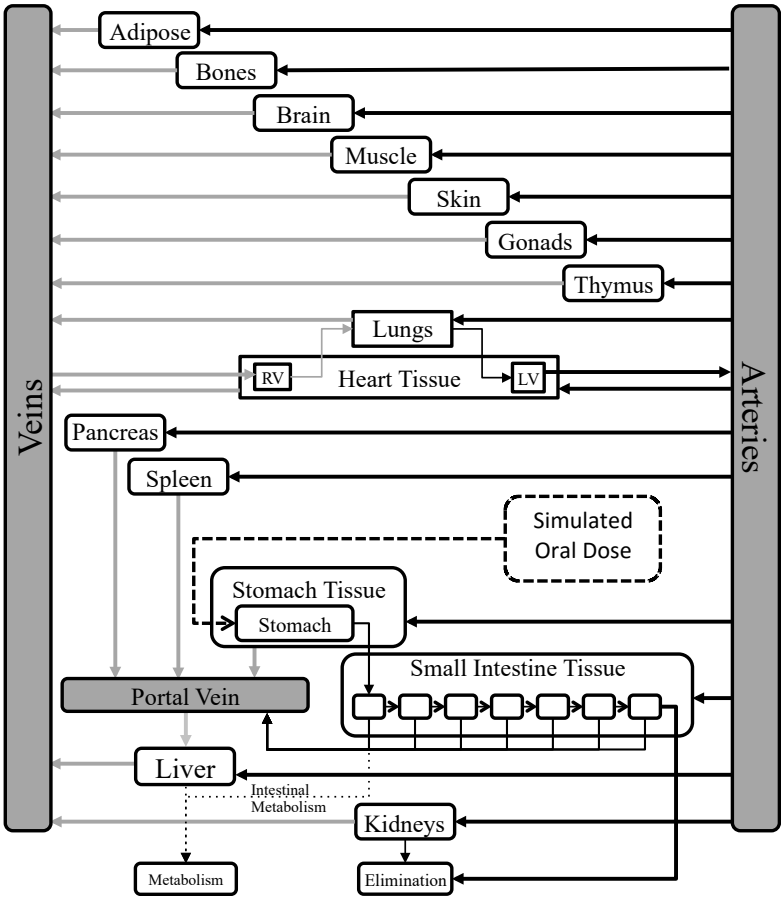

Figure 1 shows a diagram of the full body PBPK model. Figure adapted with authors permission (18).

Briefly, the equations required to simulate factors such as volume of distribution were previously published. Physicochemical properties of efavirenz data (including log P, molecular weight, pKa) and *in vitro* data (permeation across Caco-2 cells and protein binding) were gathered from the literature and incorporated into the full body model (19). Volume of distribution was simulated using the Poulin and Theil equation (20). This method describes the tissue to plasma ratio based on the individual organ volumes generated from the physB equations. Elimination clearance was calculated (using equation 1) using allometric scaling of metabolism of efavirenz in microsomes and accounting

for activity and abundance of cytochrome P450 (CYP) 2B6, CYP2A6, CYP1A2, CYP3A4 and CYP3A5, and UGT2B7.

1. $TCL_{int} = Abundance \times Liver\ weight \times MPPGL$

Where abundance is the amount of enzyme expressed per microgram of microsomal protein and MPPGL is the amount of microsomal protein per gram of liver. Apparent clearance was calculated expressed as the product of the TCL_{int} of all the enzymes contributing to the metabolism of efavirenz. Systemic clearance was calculated using equation 2, where Q_{hv} is the hepatic flow rate and *fu* is the fraction unbound in plasma (18).

2. $CL = \frac{Q_{hv} \times fu \times CL_{app}}{Q_{hv} + CL_{app} \times fu}$

The CNS portion of the model was based on validated parameters describing CNS and CSF physiology and anatomy (14). A schematic of this model is shown in Figure 2. Physiological and physicochemical properties used are displayed in Table 1. The equations used in the model presented here are as follows:

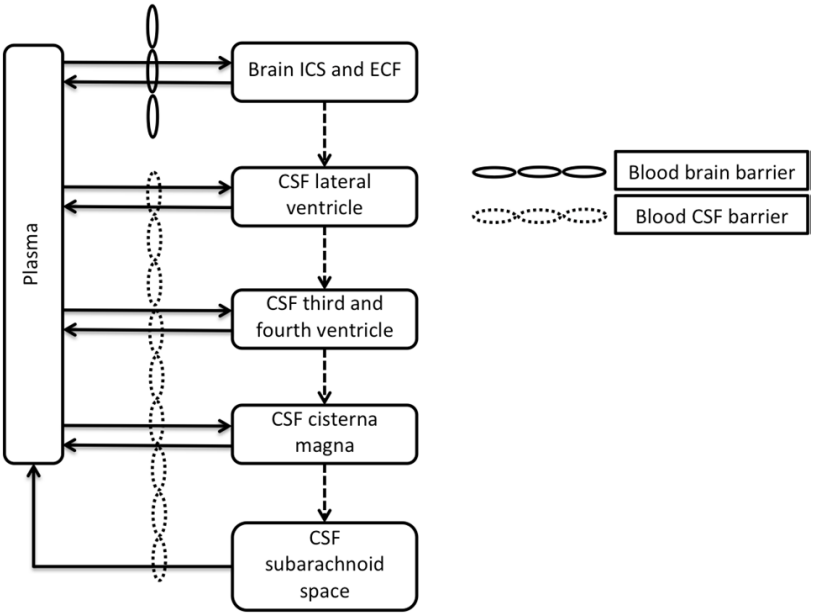

Figure 2 shows a diagram of the CNS component of the PBPK model to describe efavirenz movement within the CNS. The brain compartment is comprised of the total volume of extra cellular fluid (ECF) and intracellular space (ICS).

The equations used in the model presented here are as follow:

3. $logPS = -2.19 + 0.262\ logD + 0.0583\ vas_{base} - 0.00897\ TPSA$

Equation 3 shows a 3-descriptor QSAR model of permeability surface area product (log PS) of the blood brain barrier (BBB) developed by Liu *et al.* (21). The three descriptors are logD (octanol/water partition coefficient at pH 7.4), vas_{base} (van der Waals surface area of the basic atoms) and TPSA (van der Waals polar surface area). Permeability surface area product of the blood CSF barrier was calculated by dividing the permeability surface area product of the BBB by 1000, to reflect the smaller surface area of the blood CSF barrier (22).

4. $\frac{\Delta EFV_{Br}}{\Delta t} = psb * \left(\frac{EFV_{Ar} * fu}{R} - EFV_{Br} * fu_{Br}\right) - Q_{ecf} * EFV_{Br} * fu_{Br}$

Equation 4 describes the movement of efavirenz from arterial plasma to the brain where concentration of arterial efavirenz (EFV_{Ar}), fraction unbound in plasma (fu), blood to plasma ratio (R), concentration of efavirenz in the brain (EFV_{Br}), flow of brain extracellular fluid (Q_{ecf}), and fraction unbound in brain (fu_{Br}).

5. $\frac{\Delta EFV_{CSF\,LV}}{\Delta t} = pse * \left(\frac{EFV_{Ve} * fu}{R}\right) - pse * EFV_{LV} * fu_{CSF} + Q_{ecf} * EFV_{Br} * fu_{Br} - Q_{csf} * EFV_{LV}$

6. $\frac{\Delta EFV_{CSF\,TFV}}{\Delta t} = pse * \left(\frac{EFV_{Ve} * fu}{R}\right) - pse * EFV_{TFV} * fu_{CSF} + Q_{csf} * EFV_{LV} - Q_{csf} * EFV_{TFV}$

7. $\frac{\Delta EFV_{CSF\,CM}}{\Delta t} = pse * \left(\frac{EFV_{Ve} * fu}{R}\right) - pse * EFV_{CM} * fu_{CSF} + Q_{CSF} * EFV_{TFV} - Q_{csf} * EFV_{CM}$

8. $\frac{\Delta EFV_{CSF\,SAS}}{\Delta t} = Q_{csf} * EFV_{CM} - Q_{csf} * EFV_{SAS}$

Equations 5 to 8 describe the movement of efavirenz from the brain to CSF, including movement across the blood CSF barrier. The CSF is subdivided into 4 compartments left ventricle (LV), third and fourth ventricle (TFV), cisterna magna (CM) and the subarachnoid space (SAS) where concentration of efavirenz in veins (EFV_{Ve}), fraction unbound in plasma (fu), blood to plasma ratio (R), concentration of efavirenz in the brain (EFV_{Br}), concentration of efavirenz in the CSF compartments (EFV_{CSF}), flow of brain extracellular fluid (Q_{ecf}), flow of CSF (Q_{csf}), fraction unbound in CSF (fu_{CSF}) and fraction unbound in brain (fu_{Br}).

Simulation Design

A virtual cohort of 100 patients was generated and a once-daily dose of efavirenz (600 mg) was simulated over 5 weeks. Patient age (minimum 18 maximum 60), weight (minimum 40kg, maximum 100kg), height (minimum 1.5 meters maximum 2.1 meters) and body mass index (minimum 18, maximum 30) were generated from random normally distributed values. The PK in plasma, CSF and brain tissue were recorded during the final 24 hours at steady state. Plasma and CSF PK simulations were compared with previous data generated from clinical trials. Brain tissue to plasma ratios were also calculated and compared to data generated in rodents.

Materials

Male Wistar rats were purchased from Charles River (Oxford, UK). Efavirenz powder (>98% pure) was purchased from LGM Pharma Inc (Boca Raton, USA). All other consumables were purchased from Sigma Aldrich (Dorset, UK).

Results

The protein binding of efavirenz in brain tissue was determined using rapid equilibrium dialysis. The mean (± standard deviation) concentration of efavirenz detected in the receiver chamber was 209.7 ± 33.4 ng mL^{-1}, and 165 ± 22.0 ng mL^{-1} 10% and 20% brain homogenate respectively. The fraction unbound in brain tissue (fu_{Br}) was calculated to be 0.00181 and 0.00212 in 10% and 20% brain homogenate, respectively. The average fu_{Br} was 0.00197.

Following 5 weeks of oral dosing of efavirenz (10 mg kg^{-1}), the median plasma concentration of efavirenz in rats was 69.7 ng mL^{-1} (IQR 44.9 – 130.6). Median efavirenz concentrations in brain tissue were 702.9 ng mL^{-1} (IQR 475.5 – 1018.0). The median tissue to plasma ratio was 9.5 (IQR 7.0 – 10.9).

Simulation

A standard dosing schedule of efavirenz (600 mg once daily) was simulated in 100 patients for the duration of 5 weeks. The results for efavirenz concentrations in plasma (Figure 3A), CSF (Figure 3B) and brain tissue (Figure 3C) were all taken from the final 24 hours of the simulation.

Antimicrobial Agents and Chemotherapy

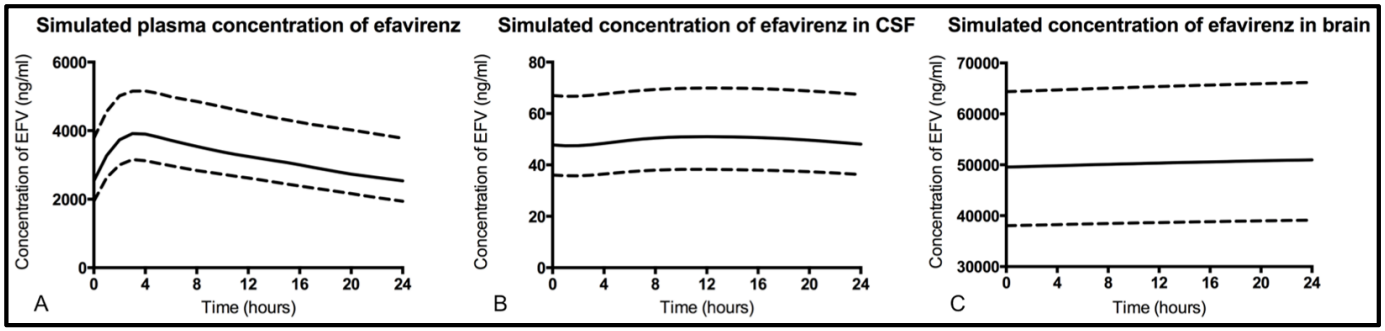

Figure 3 shows the median (solid line) simulated plasma (a), CSF (b) and brain tissue (c) concentrations of efavirenz during the final 24 hours following 5 weeks of once daily efavirenz (600mg). Also shown is the interquartile range (dotted line).

The maximum concentration (C_{max}), minimum concentration (C_{min}) and area under the curve (AUC_{24}) of efavirenz in plasma were 3916 ng mL^{-1} (IQR 3155-5153), 2537 ng mL^{-1} (IQR 1942-3779) and 76,991 ng.h mL^{-1} (IQR 62,170-107,560). The CSF was predicted to have lower concentrations of efavirenz C_{max} 50.96 ng mL^{-1} (IQR 38.23-69.09), C_{min} 47.8 ng mL^{-1} (IQR 36.1-66.7) and AUC_{24} 1193 ng.h mL^{-1} (IQR 898-1649). At 24 hours efavirenz in the CSF was 1.6% of plasma concentrations. The simulation predicted efavirenz concentrations in the brain to exceed CSF and plasma, C_{max} 50,973 ng mL^{-1} (IQR 39,122-66,177), C_{min} 49,566 ng mL^{-1} (IQR 38,044-64,374) and AUC_{24} 1,207,542 ng.h mL^{-1} (IQR 926,900-1,567,974). The brain tissue to plasma partition ratio at 24 hours was 15.8.

The absorption constant (K_a) was predicted to be 0.19 h^{-1} (IQR, 0.18-0.21). Volume of distribution (V_{SS}) and elimination clearance (Cl) were predicted to be 2.15 l kg^{-1} (IQR 2.06-2.31) 4.56 l h^{-1} (IQR 3.52-5.33) respectively. The fraction absorbed (fa) of efavirenz was predicted to be median 0.46 (IQR, 0.44-0.49) and was used to calculate apparent V_{SS} and apparent Cl, 323.31 l^{-1} (IQR 308.31-346.28) and 9.79 l h^{-1} (7.54-11.41) respectively.

Comparison with clinical data

The simulated PK parameters in plasma produced by the model were in agreement with data published from human trials and population PK studies (popPK). Table 2 shows the results from the simulation and a number of clinical studies and popPK studies. The mean/median observed plasma concentrations of EFV ranged from 1973 ng mL^{-1} to 3180 ng mL^{-1} (9, 23-26). Simulated Cl, V_{SS} and K_a were 1.04 fold, 1.28 fold and 0.6 fold different compared to observed data (26). The average simulated CSF concentrations were 49.9 ng mL^{-1} (IQR 36.6-69.7) compared to a range of 11.1 ng mL^{-1} to 16.3 ng mL^{-1} observed in previously published clinical studies (9, 23).

Discussion

The presented data show that the PBPK model predicts efavirenz to accumulate in the brain in concentrations that far exceed those in the CSF. Human CSF concentrations were gathered from relatively small cohorts (Best N=80, Yilmaz N=1 and Tashima N=10) and may not fully represent CSF concentrations larger populations. Indeed, concentrations of efavirenz in the brain were predicted to exceed even plasma concentrations, with a brain to plasma ratio of 15.8. The rodent data presented here supports the model prediction of a higher concentration of efavirenz in brain tissue, with a median tissue to plasma ratio of 9.5. Recently, efavirenz has been demonstrated to accumulate in the brain tissue of a macaque. Following 8 days of orally administered efavirenz (60 mg kg^{-1}) the concentrations in plasma and CSF were 541 and 3.30 ng mL^{-1} respectively. Concentrations of efavirenz in the cerebellum and basal ganglia were 6.86 µg g^{-1} (tissue to plasma ratio 12.7) and 2.01 µg g^{-1} (tissue to plasma ratio 3.7) respectively (27).

Currently only one study has examined efavirenz concentrations in human brain tissue (28). This study showed similar brain concentrations to historical CSF values and are in disagreement with the data presented here. While participants in this analysis had efavirenz detectable in intracardiac serum using a qualitative assay, reliable dosing information was not routinely available since the final care setting varied between individuals (home, hospice, or hospital). Given this uncertainty regarding the final dosing interval, no precise information was available on the time of last dose, which complicates interpretation of the reported brain concentrations. If the last efavirenz dose was administered, for example, 3 days prior to death, then the brain tissue concentrations may not accurately reflect those that occur in living, adherent patients. However, efavirenz has been shown to display long plasma half-life (40 to 52 hours) (29). This would indicate patients would have had ceased receiving efavirenz for many days or having poor adherence in order to explain the very low concentrations observed. Despite this the data predicted by the model is supported by robust data generated from the brain tissue concentrations from rats and monkeys (27).

341 Accumulation of efavirenz in brain tissue may be driven by physicochemical properties of efavirenz,
342 in particular lipophilicity. Since efavirenz is highly lipophilic (logP 4.6) and has high accumulation
343 in multiple cell types, it shows high cellular permeation (19). The brain has a high fat content, with
344 approximately 60% of the brain consisting of fat (30). An additional factor that favours distribution
345 is the high degree of protein binding of efavirenz. In plasma, efavirenz is highly protein bound (fu
346 0.01) (31). Protein binding in the CSF is much lower leading to more free efavirenz, fu 0.238 (29).
347 The data presented here from rapid equilibrium dialysis shows efavirenz fu in rodent brain tissue to
348 be 0.00197. Taken collectively, the combination of low fu and affinity for the lipophilic environment
349 of the brain favour accumulation of efavirenz in the CNS. Lipophilicity has been shown to be a
350 significant factor in uptake of drugs into the brain (32). Lipophilicity, but not plasma protein binding,
351 was shown to correlate with uptake of benzodiazepines, for example, into the brain. However, this
352 study did not consider fu in the brain and plasma fu may not be a good indicator of brain fu. Kalvass
353 *et al* examined the fu in plasma and brain tissue of 34 drugs covering multiple drug classes. The data
354 presented showed that plasma fu both under and overestimated brain fu depending on the drug (33).
355
356 Although this is the first study to employ PBPK modelling to investigate efavirenz distribution into
357 the CNS, PBPK has been used previously to investigate efavirenz dose optimisation, drug-drug
358 interactions and PK in special populations (19, 34).
359
360 Limitations of this work include that the presented model does not take into account genetic
361 variability (i.e. *CYP2B6* variants), the brain fu values were generated in rodent brain rather than
362 human brain, the current model is not able to estimate local concentrations in individual brain
363 regions, and permeability of efavirenz was calculated using a QSAR model of passive permeability
364 which often rely on extrapolated data from animals with important differences to humans (21, 35).
365 The CSF concentrations predicted by the model were approximately 3 fold greater than observed in
366 human patients. This indicates that the interactions with efavirenz and the blood CSF barrier may not
367 have been accurately represented. The permeability of efavirenz at the blood CSF barrier was

adjusted for the decreased surface area of the blood CSF barrier, 1000 times less than the BBB (22). The assumption that the permeability of the two barriers is equal may be incorrect. However, these aspects could be expanded in future modelling strategies as the necessary input data emerges.

The BBB is highly effective at excluding xenobiotics from the CNS. Tight cellular junctions prevent paracellular transport of drugs and the metabolising enzymes and transport proteins remove drugs from the CNS. As such, another potential limitation of the model that warrants further elaboration is that distribution of efavirenz across the BBB may not be governed purely by passive permeability. The potential influence of influx and efflux transporters was not considered because efavirenz is not classified as substrate of any transporters and effects of transporters on efavirenz PK have not been described. The model presented here potentially may be improved upon in the future if efavirenz is demonstrated to be a substrate for such transporters.

Numerous studies have linked efavirenz plasma concentrations to clinical evidence of CNS toxicity. Other studies have shown that efavirenz readily passes the BBB and is present in CSF. The simulations presented here indicate plasma and CSF may underestimate efavirenz exposure within the brain. Limitations associated with obtaining tissue biopsies and paired plasma and CSF samples from patients make PBPK modelling an attractive tool for estimating such drug distribution.

Author Contributions

P.C., R.K.R.R., D.M.M., N.J.L., S.L., A.O. and M.S. wrote the manuscript.

P.C., and M.S. designed research.

P.C., R.K.R.R., D.M.M. and N.J.L. performed research.

P.C., R.K.R.R. and M.S. analysed data.

Conflict of Interst/Disclosure

S. Letendre is funded by NIH research awards, including HHSN271201000036C, R01 MH58076, R01 MH92225, P50 DA26306, and P30 MH62512. He has received support for research projects

from Abbott, Merck, Tibotec, and GlaxoSmithKline. He has consulted for Gilead Sciences, GlaxoSmithKline, Merck, and Tibotec and has received lecture honoraria from Abbott and Boehringer-Ingelheim. Andrew Owen has received research funding from Merck, Pfizer and AstraZeneca, consultancy from Merck and Norgine, and is a co-inventor of patents relating to HIV nanomedicines. Marco Siccardi has received research funding from ViiV and Janssen.

References

1. **Sanchez Martin A, Cabrera Figueroa S, Cruz Guerrero R, Hurtado LP, Hurle AD, Carracedo Alvarez A.** 2013. Impact of pharmacogenetics on CNS side effects related to efavirenz. Pharmacogenomics **14:**1167-1178.
2. **Vrouenraets SM, Wit FW, van Tongeren J, Lange JM.** 2007. Efavirenz: a review. Expert Opin Pharmacother **8:**851-871.
3. **Leutscher PD, Stecher C, Storgaard M, Larsen CS.** 2013. Discontinuation of efavirenz therapy in HIV patients due to neuropsychiatric adverse effects. Scand J Infect Dis **45:**645-651.
4. **Theys K, Camacho RJ, Gomes P, Vandamme AM, Rhee SY, Portuguese HIVRSG.** 2015. Predicted residual activity of rilpivirine in HIV-1 infected patients failing therapy including NNRTIs efavirenz or nevirapine. Clin Microbiol Infect **21:**607 e601-608.
5. **Fumaz CR, Tuldra A, Ferrer MJ, Paredes R, Bonjoch A, Jou T, Negredo E, Romeu J, Sirera G, Tural C, Clotet B.** 2002. Quality of life, emotional status, and adherence of HIV-1-infected patients treated with efavirenz versus protease inhibitor-containing regimens. J Acquir Immune Defic Syndr **29:**244-253.
6. **Perez-Molina JA.** 2002. Safety and tolerance of efavirenz in different antiretroviral regimens: results from a national multicenter prospective study in 1,033 HIV-infected patients. HIV Clin Trials **3:**279-286.
7. **Wyen C, Hendra H, Siccardi M, Platten M, Jaeger H, Harrer T, Esser S, Bogner JR, Brockmeyer NH, Bieniek B, Rockstroh J, Hoffmann C, Stoehr A, Michalik C, Dlugay V, Jetter A, Knechten H, Klinker H, Skaletz-Rorowski A, Fatkenheuer G, Egan D, Back DJ, Owen A, German Competence Network for HIVAC.** 2011. Cytochrome P450 2B6 (CYP2B6) and constitutive androstane receptor (CAR) polymorphisms are associated with early discontinuation of efavirenz-containing regimens. J Antimicrob Chemother **66:**2092-2098.
8. **Marzolini C, Telenti A, Decosterd LA, Greub G, Biollaz J, Buclin T.** 2001. Efavirenz plasma levels can predict treatment failure and central nervous system side effects in HIV-1-infected patients. AIDS **15:**71-75.
9. **Best BM, Koopmans PP, Letendre SL, Capparelli EV, Rossi SS, Clifford DB, Collier AC, Gelman BB, Mbeo G, McCutchan JA, Simpson DM, Haubrich R, Ellis R, Grant I, Group C.** 2011. Efavirenz concentrations in CSF exceed IC50 for wild-type HIV. J Antimicrob Chemother **66:**354-357.
10. **Gibbs JE, Gaffen Z, Thomas SA.** 2006. Nevirapine uptake into the central nervous system of the Guinea pig: an in situ brain perfusion study. J Pharmacol Exp Ther **317:**746-751.
11. **Blaney SM, Daniel MJ, Harker AJ, Godwin K, Balis FM.** 1995. Pharmacokinetics of lamivudine and BCH-189 in plasma and cerebrospinal fluid of nonhuman primates. Antimicrob Agents Chemother **39:**2779-2782.

12. **Shen DD, Artru AA, Adkison KK.** 2004. Principles and applicability of CSF sampling for the assessment of CNS drug delivery and pharmacodynamics. Adv Drug Deliv Rev **56:**1825-1857.
13. **Bosgra S, van Eijkeren J, Bos P, Zeilmaker M, Slob W.** 2012. An improved model to predict physiologically based model parameters and their inter-individual variability from anthropometry. Crit Rev Toxicol **42:**751-767.
14. **Westerhout J, Ploeger B, Smeets J, Danhof M, de Lange EC.** 2012. Physiologically based pharmacokinetic modeling to investigate regional brain distribution kinetics in rats. AAPS J **14:**543-553.
15. **O'Mahony SM, Myint AM, Steinbusch H, Leonard BE.** 2005. Efavirenz induces depressive-like behaviour, increased stress response and changes in the immune response in rats. Neuroimmunomodulation **12:**293-298.
16. **Liu X, Van Natta K, Yeo H, Vilenski O, Weller PE, Worboys PD, Monshouwer M.** 2009. Unbound drug concentration in brain homogenate and cerebral spinal fluid at steady state as a surrogate for unbound concentration in brain interstitial fluid. Drug Metab Dispos **37:**787-793.
17. **Kalvass JC, Maurer TS.** 2002. Influence of nonspecific brain and plasma binding on CNS exposure: implications for rational drug discovery. Biopharm Drug Dispos **23:**327-338.
18. **Rajoli RK, Back DJ, Rannard S, Freel Meyers CL, Flexner C, Owen A, Siccardi M.** 2015. Physiologically Based Pharmacokinetic Modelling to Inform Development of Intramuscular Long-Acting Nanoformulations for HIV. Clin Pharmacokinet **54:**639-650.
19. **Siccardi M, Almond L, Schipani A, Csajka C, Marzolini C, Wyen C, Brockmeyer NH, Boffito M, Owen A, Back D.** 2012. Pharmacokinetic and pharmacodynamic analysis of efavirenz dose reduction using an in vitro-in vivo extrapolation model. Clin Pharmacol Ther **92:**494-502.
20. **Poulin P, Theil FP.** 2002. Prediction of pharmacokinetics prior to in vivo studies. 1. Mechanism-based prediction of volume of distribution. J Pharm Sci **91:**129-156.
21. **Liu X, Tu M, Kelly RS, Chen C, Smith BJ.** 2004. Development of a computational approach to predict blood-brain barrier permeability. Drug Metab Dispos **32:**132-139.
22. **Pardridge WM.** 2002. Drug and gene delivery to the brain: the vascular route. Neuron **36:**555-558.
23. **Yilmaz A, Watson V, Dickinson L, Back D.** 2012. Efavirenz pharmacokinetics in cerebrospinal fluid and plasma over a 24-hour dosing interval. Antimicrob Agents Chemother **56:**4583-4585.
24. **Tashima KT, Caliendo AM, Ahmad M, Gormley JM, Fiske WD, Brennan JM, Flanigan TP.** 1999. Cerebrospinal fluid human immunodeficiency virus type 1 (HIV-1) suppression and efavirenz drug concentrations in HIV-1-infected patients receiving combination therapy. J Infect Dis **180:**862-864.
25. **Sanchez A, Cabrera S, Santos D, Valverde MP, Fuertes A, Dominguez-Gil A, Garcia MJ, Tormes G.** 2011. Population pharmacokinetic/pharmacogenetic model for optimization of efavirenz therapy in Caucasian HIV-infected patients. Antimicrob Agents Chemother **55:**5314-5324.
26. **Csajka C, Marzolini C, Fattinger K, Decosterd LA, Fellay J, Telenti A, Biollaz J, Buclin T.** 2003. Population pharmacokinetics and effects of efavirenz in patients with human immunodeficiency virus infection. Clin Pharmacol Ther **73:**20-30.
27. **Thompson CG, Bokhart MT, Sykes C, Adamson L, Fedoriw Y, Luciw PA, Muddiman DC, Kashuba AD, Rosen EP.** 2015. Mass spectrometry imaging reveals heterogeneous efavirenz distribution within putative HIV reservoirs. Antimicrob Agents Chemother **59:**2944-2948.
28. **Namandje Bumpus QM, Brookie Best, David Moore, Ronald J. Ellis, Melanie Crescini, Cristian Achim, Courtney Fletcher, Eliezer Masliah, Igor Grant, and Scott**

Letendre for the CNTN Group. Antiretroviral Concentrations in Brain Tissue Are Similar to or Exceed Those in CSF, p. *In* (ed),

29. **Avery LB, Sacktor N, McArthur JC, Hendrix CW.** 2013. Protein-free efavirenz concentrations in cerebrospinal fluid and blood plasma are equivalent: applying the law of mass action to predict protein-free drug concentration. Antimicrob Agents Chemother **57:**1409-1414.
30. **Chang CY, Ke DS, Chen JY.** 2009. Essential fatty acids and human brain. Acta Neurol Taiwan **18:**231-241.
31. **Almond LM, Hoggard PG, Edirisinghe D, Khoo SH, Back DJ.** 2005. Intracellular and plasma pharmacokinetics of efavirenz in HIV-infected individuals. J Antimicrob Chemother **56:**738-744.
32. **Pajouhesh H, Lenz GR.** 2005. Medicinal chemical properties of successful central nervous system drugs. NeuroRx **2:**541-553.
33. **Kalvass JC, Maurer TS, Pollack GM.** 2007. Use of plasma and brain unbound fractions to assess the extent of brain distribution of 34 drugs: comparison of unbound concentration ratios to in vivo p-glycoprotein efflux ratios. Drug Metab Dispos **35:**660-666.
34. **Siccardi M, Olagunju A, Seden K, Ebrahimjee F, Rannard S, Back D, Owen A.** 2013. Use of a physiologically-based pharmacokinetic model to simulate artemether dose adjustment for overcoming the drug-drug interaction with efavirenz. In Silico Pharmacol **1:**4.
35. **Zimmermann C, van de Wetering K, van de Steeg E, Wagenaar E, Vens C, Schinkel AH.** 2008. Species-dependent transport and modulation properties of human and mouse multidrug resistance protein 2 (MRP2/Mrp2, ABCC2/Abcc2). Drug Metabolism and Disposition **36:**631-640.

Model Parameter	Value	Reference
Molecular Weight	315.7	(19)
LogP	4.6	(19)
pKa	10.2	(19)
Caco-2 permiability (10^{-6} cm/s)	2.5	(19)
Fraction unbound		
Plasma	0.01	(31)
CSF	0.238	(29)
Brain tissue	0.00197	
PSB	2.47	
PSE	0.00247	
Qcsf (mL/min)	0.175	(14)
Qecf (mL/min)	0.4	(14)
Brain ICS (mL)	960	(14)
Brain ECF (mL)	240	(14)
CSF LV (mL)	22.5	(14)
CSF TFV (mL)	22.5	(14)
CSF CM (mL)	7.5	(14)
CSF SAS (mL)	90	(14)

530

531 **Table 1** shows the physiological and physicochemical variables used to generate the PBPK model.

532 Intracellular space (ICS), extra cellular fluid (ECF), left ventricle (LV), third and fourth ventricles

533 (TFV), cisterna magna (CM) and sub arachnoid space (SAS).

	Simulated data		Yilmaz *et al* 2012* (22)	Best *et al* 2011 (9)	Tashima *et al* 1999 (23)	Sánchez *et al* 2011 (24)	Csajka *et al* 2003 (25)
	Mean	Median	Median	Median	Mean	Mean	Mean
Plasma concentration (ng ml^{-1})	3183 (SD ±447)	3184 (IQR 2219-4851)	3718 (range 2439-4952)	2145 (IQR 1384-4423)	1973.8 (range 792.2-2950.9)	3180 (SD ±1610)	
Plasma AUC (ng.h mL^{-1})	91924 (SD ±51619)	76991 (IQR 62170-107560)	86,280				
Apparent Cl (L h^{-1})	9.29 (SE ±0.26)	9.79 (IQR 7.54-11.44)				9.61 (SE ±0.38)	9.4 (SE ±0.36)
Aparent V_{SS} (L kg^{-1})	329.43 (SE ±2.38)	323.31 (IQR 308.31-346.28)				291 (SE ±44.81)	252 (SE ±35.28)
K_a (h^{-1})	0.20 (SD ±0.02)	0.19 (IQR 0.18-0.21)					0.3 (SE ±0.09)
CSF concentration (ng mL^{-1})	49.9 (SD ±1.2)	49.9 (IQR 36.6-69.7)	16.3 (range 7.3-22.3)	13.9 (IQR 4.1-21.2)	11.1 (SD 2.1-18.6)		
CSF AUC (ng.h mL^{-1})	1401 (SD ±809)	1193 (IQR 898-1649)	380				
Brain tissue concentration (ng mL^{-1})	50312.5 (SD ±438)	50343 (IQR 38351-65799)					
Brain tissue AUC (ng.h mL^{-1})	1397820 (SD ±815657)	1207542 (IQR 926900-1567974)					

Table 2 shows the results from the simulation and a number of human trials and POP PK studies. Results are presented as either mean (± standard deviation [SD] or standard error [SE]) or median (± interquartile range [IQR]). Mean and median are presented to allow comparison of simulated and clinical. * all samples in this study were obtained from a single patient over 24 hours.

Antimicrobial Agents and Chemotherapy